**Journal of Diabetes Science and Technology**
Volume 2, Issue 4, July 2008


ORIGINAL ARTICLES

# A Subcutaneous Insulin Pharmacokinetic Model for Computer Simulation in a Diabetes Decision Support Role: Model Structure and Parameter Identification

Jason Wong, B.Eng,[1] J. Geoffrey Chase, Ph.D.,[1] Christopher E. Hann, Ph.D.,[1] Geoffrey M. Shaw, MBChB, FJFICM,[2] Thomas F. Lotz, Dipl. Ing, Ph.D.,[1] Jessica Lin, B.Eng, Ph.D.,[1] and Aaron J. Le Compte, B.Eng[1]

## Abstract

***Objective:***
The goal of this study was to develop a unified physiological subcutaneous (SC) insulin absorption model for computer simulation in a clinical diabetes decision support role. The model must model the plasma insulin appearance of a wide range of current insulins, especially monomer insulin and insulin glargine, utilizing common chemical states and transport rates, where appropriate.

***Methods:***
A compartmental model was developed with 13 patient-specific model parameters covering six diverse insulin types [rapid-acting, regular, neutral protamine Hagedorn (NPH), lente, ultralente, and glargine insulin]. Model parameters were identified using 37 sets of mean plasma insulin time-course data from an extensive literature review via nonlinear optimization methods.

***Results:***
All fitted parameters have a coefficient of variation <100% (median 51.3%, 95th percentile 3.6–60.6%) and can be considered a posteriori identifiable.

***Conclusion:***
A model is presented to describe SC injected insulin appearance in plasma in a diabetes decision support role. Clinically current insulin types (monomeric insulin, regular insulin, NPH, insulin, and glargine) and older insulin types (lente and ultralente) are included in a unified framework that accounts for nonlinear concentration and dose dependency. Future work requires clinical validation using published pharmacokinetic studies.

*J Diabetes Sci Technol 2008;2(4):658-671*

**Author Affiliations:** [1]Department of Mechanical Engineering, University of Canterbury, Christchurch, New Zealand, and [2]Department of Intensive Care, Christchurch Hospital, Christchurch School of Medicine and Health Science, University of Otago, Dunedin, New Zealand

**Abbreviations:** (CV) coefficient of variation, (MI) monomeric insulin, (NLS) nonlinear least squares, (NPH) neutral protamine Hagedorn, (PK) pharmacokinetic, (RI) regular insulin, (SC) subcutaneous, (SSE) sum squared error

**Keywords:** blood glucose, compartmental models, decision support, diabetes, hyperglycemia, insulin, simulation, subcutaneous injection

**Corresponding Author:** Jason Wong, Department of Mechanical Engineering, University of Canterbury, Private Bag 4800, Christchurch, New Zealand; email address xww10@student.canterbury.ac.nz

## Introduction

For more than 80 years, administration of insulin via the subcutaneous (SC) route into the peripheral circulation has been the most widely used therapy in ambulatory diabetes. Since Binder,[1] the absorption kinetics of subcutaneously injected insulin has emerged as a mature research field.[2–4] Insulin absorption kinetics are complex and can be influenced in many complex ways. Insulin-independent factors include SC blood flow (which can be influenced by temperature,[2,5] exercise,[6,7] and even smoking[8,9]), depth of injection,[10,11] and site of injection.[4] There are also insulin-dependent factors, which include the species of insulin[12] and the concentration and volume of injected insulin.[1,4,10,13] As a result, SC insulin pharmacokinetics (PK) are variable enough to offer significant practical difficulties in providing consistent therapy for diabetes. Most studies report interindividual variation in key pharmacokinetic summary measures from 15[14] to 107%,[4] depending on insulin type.

Some diabetes decision support and control methods[15–18] rely on SC absorption models to deterministically predict plasma insulin appearance from SC injection, thus tracking on-board insulin from multiple doses over extended periods. Some would argue the clinical value to general diabetes management of such models given the inherent and significant intra- and interpatient variability in absorption.[14,19–23]

Nevertheless, given the often limited data available for glycemic control in diabetes,[24,25] the qualitative estimation of the plasma insulin time course is not only useful but necessary for efficient dosing and reduced risk of hypoglycemia. Deterministic models of absorption can also form the basis of stochastic methods, as hinted at by Andreassen and colleagues[18] with significant potential. These models have also proven useful for glycemic control simulation[15,18,26] and diabetes education.[27]

Previous work in insulin PK modeling is voluminous. Kobayashi and associates[28] experimented with single- and dual-compartment models for regular insulin (RI) absorption. As most current regular insulin is regular human insulin, the term regular insulin in this study is taken to mean regular human insulin. Later, Kraegen *et al.*[29,30] developed a three-compartment model, which was refined with a minimal approach by Puckett *et al.*,[31] modeling the long-acting ultralente insulin as an unlikely continuous flow in addition to RI. As the use of monomeric insulin (MI) types matured clinically, more models concentrated on its absorption kinetics. In this study and elsewhere, the term "monomeric insulin" is a convenient misnomer used for rapid-acting insulin analogues whose hexamers dissociate very rapidly into dimers/monomers in subcutaneous tissue, resulting in a monoexponential decay curve.[32] With a similar three-compartment model, Shimoda *et al.*[17] modeled both RI and MI absorption. More recently, Wilinska *et al.*[33] demonstrated a four-compartment model of MI absorption with fast/slow absorption channels and local insulin degradation.

All these models apply to prandial insulin only, which is limiting, as basal-acting insulin is required in ~90% of all insulin-dependent diabetics not on insulin pump therapy (calculated based on estimated insulin pump use[34] and prevalence of diabetes[35] 2003 and 2005 statistics, U.S. figures only). The absorption dependency of RI on dose, concentration, and volume is also not modeled by any of these simpler compartmental models as noted earlier.

Noncompartmental approaches include Berger and Rodbard,[26] whose simulation model has been adopted by the AIDA decision support system.[36] A three-parameter logistic equation with linear dose dependency is used to describe the SC insulin plasma rate of appearance, while a two-compartment model describes plasma insulin kinetics and action. A wide range of older insulin types [e.g., RI, neutral protamine Hagedorn (NPH), lente, and ultralente] have been modeled and remain the only model for NPH-type insulins. While this model accounts for general dose dependency of absorption, it does not account for the underlying volume or concentration effects.

The model by Mosekilde *et al.*[13] describes the absorption kinetics with coupled partial differential equations of detailed physicochemical properties of insulin. While accounting for dose, volume, and concentration dependency, solving the nonlinear-coupled differential equations it employs is computationally burdensome and only RI is modeled. This model was simplified by Trajanoski *et al.*[37] and subsequently extended by Tarin *et al.*[38] to insulin glargine, a long-acting basal insulin analogue, and is currently the only model for this newer insulin. While these noncompartmental models are more physiological than the compartmental models, the associated computational cost can be prohibitive,

especially if the intended or potential end use is a real-time diabetes decision support system.

In summary, the complex, noncompartmental models better capture some published insulin absorption kinetics, while the computationally minimal compartmental models better suit simulation in a real-time diabetes decision support system. The more complicated kinetics of RI have not been modeled compartmentally nor have insulin glargine or even older intermediate and long-acting insulin types such as lente and ultralente. Most existing models also describe only one insulin type or a limited number with no commonality.[17] Critical reviews of some of these models are available from Nucci and Cobelli.[39] Compartmental modeling methods are also well reviewed in Carson and Cobelli.[40]

This article developed a physiological compartment model for a wide range of insulin types. Specifically, fast- and short-acting prandial insulins (MI and RI) and intermediate- and long-acting basal insulins (NPH, lente, ultralente, and insulin glargine) are modeled. The main principle was to more accurately capture the main dynamics of the absorption kinetics with a compartmental model using first-order kinetics. The secondary goal was to provide a computationally minimal, yet consistent, physiologically unified framework for all insulin types. The model also accounts for volume and concentration dependency on SC absorption of human insulins. The intended end use is as a simulation model for a real-time decision support system.

## Methods

A diagram of the structure of the SC insulin absorption kinetic model is shown in **Figure 1**. The model equations are then listed, followed by a description of the individual sections of the model for each insulin type. After this description, a summary of the model is presented.

Hexameric state: common to RI, NPH, and lente insulin types

$$\dot{x}_h(t) = -(k_1 + k_d)x_h(t) + k_{crys,NPH}c_{NPH}(t) + k_{crys,len}c_{len}(t) + u_{h,RH}(t) + u_{h,NPH}(t) + u_{h,len}(t) \quad (1)$$

Dimeric/monomeric state: common to all insulin types

$$\dot{x}_{dm}(t) = -(k_2 + k_d)x_{dm}(t) + k_1 x_h(t) + k_{1,ulen}x_{h,ulen}(t) + k_{1,gla}x_{h,gla}(t) + u_{mono}(t) + u_{m,RHt}(t) + u_{m,NPH}(t) + u_{m,len}(t) + u_{m,ulen}(t) + u_{m,gla}(t) \quad (2)$$

NPH and lente insulin compartments

$$\dot{c}_{NPH}(t) = -k_{crys,NPH}c_{NPH}(t) + u_{c,NPH}(t) \quad (3)$$

$$\dot{c}_{len}(t) = -k_{crys,len}c_{len}(t) + u_{c,len}(t) \quad (4)$$

Ultralente insulin compartments

$$\dot{x}_{h,ulen}(t) = -(k_{1,ulen} + k_d)x_{h,ulen}(t) + k_{crys,ulen}c_{ulen}(t) + u_{h,ulen}(t) \quad (5)$$

$$\dot{c}_{ulen}(t) = -k_{crys,ulen}c_{ulen}(t) + u_{c,ulen}(t) \quad (6)$$

Insulin glargine compartments

$$\dot{x}_{h,gla}(t) = -(k_{1,gla} + k_d)x_{h,gla}(t) + \min(k_{prep,gla}p_{gla}(t), r_{dis,\max}) + u_{h,gla}(t) \quad (7)$$

$$\dot{p}_{gla}(t) = -\min(k_{prep,gla}p_{gla}(t), r_{dis,\max}) + u_{p,gla}(t) \quad (8)$$

Mass balance insulin inputs

$$u_{total,NPH}(t) = u_{c,NPH}(t) + u_{h,NPH}(t) + u_{m,NPH}(t) \quad (9)$$

$$u_{total,len}(t) = u_{c,len}(t) + u_{h,len}(t) + u_{m,len}(t) \quad (10)$$

$$u_{total,ulen}(t) = u_{c,ulen}(t) + u_{h,ulen}(t) + u_{m,ulen}(t) \quad (11)$$

$$u_{total,gla}(t) = u_{p,gla}(t) + u_{h,gla}(t) + u_{m,gla}(t) \quad (12)$$

$$u_{total,RH}(t) = u_{h,RH}(t) + u_{m,RH}(t) \quad (13)$$

$$u_{total,mono}(t) = u_{mono}(t) \quad (14)$$

Mass input fractions and components

$$u_{c,NPH}(t) = \alpha_{NPH}u_{total,NPH}(t) \quad (15)$$

$$u_{c,len}(t) = \alpha_{len}u_{total,len}(t) \quad (16)$$

$$u_{c,ulen}(t) = \alpha_{ulen}u_{total,ulen}(t) \quad (17)$$

$$u_{p,gla}(t) = \alpha_{gla}u_{total,gla}(t) \quad (18)$$

$$u_{h,NPH}(t) + u_{m,NPH}(t) = (1 - \alpha_{NPH})u_{total,NPH}(t) \quad (19)$$

$$u_{h,len}(t) + u_{m,len}(t) = (1 - \alpha_{len})u_{total,len}(t) \quad (20)$$

$$u_{h,ulen}(t) + u_{m,ulen}(t) = (1 - \alpha_{ulen})u_{total,ulen}(t) \quad (21)$$

$$u_{h,gla}(t) + u_{m,gla}(t) = (1 - \alpha_{gla})u_{total,gla}(t) \quad (22)$$

where all variables in **Equations 1–22** are defined:

$x_h(t)$ Mass in the hexameric compartment (mU)

$x_{h,ulen}(t)$ Mass in the ultralente hexameric compartment (mU)

$x_{h,gla}(t)$ Mass in the glargine hexameric compartment (mU)

$c_{NPH}(t)$ Mass in the NPH crystalline protamine compartment (mU)

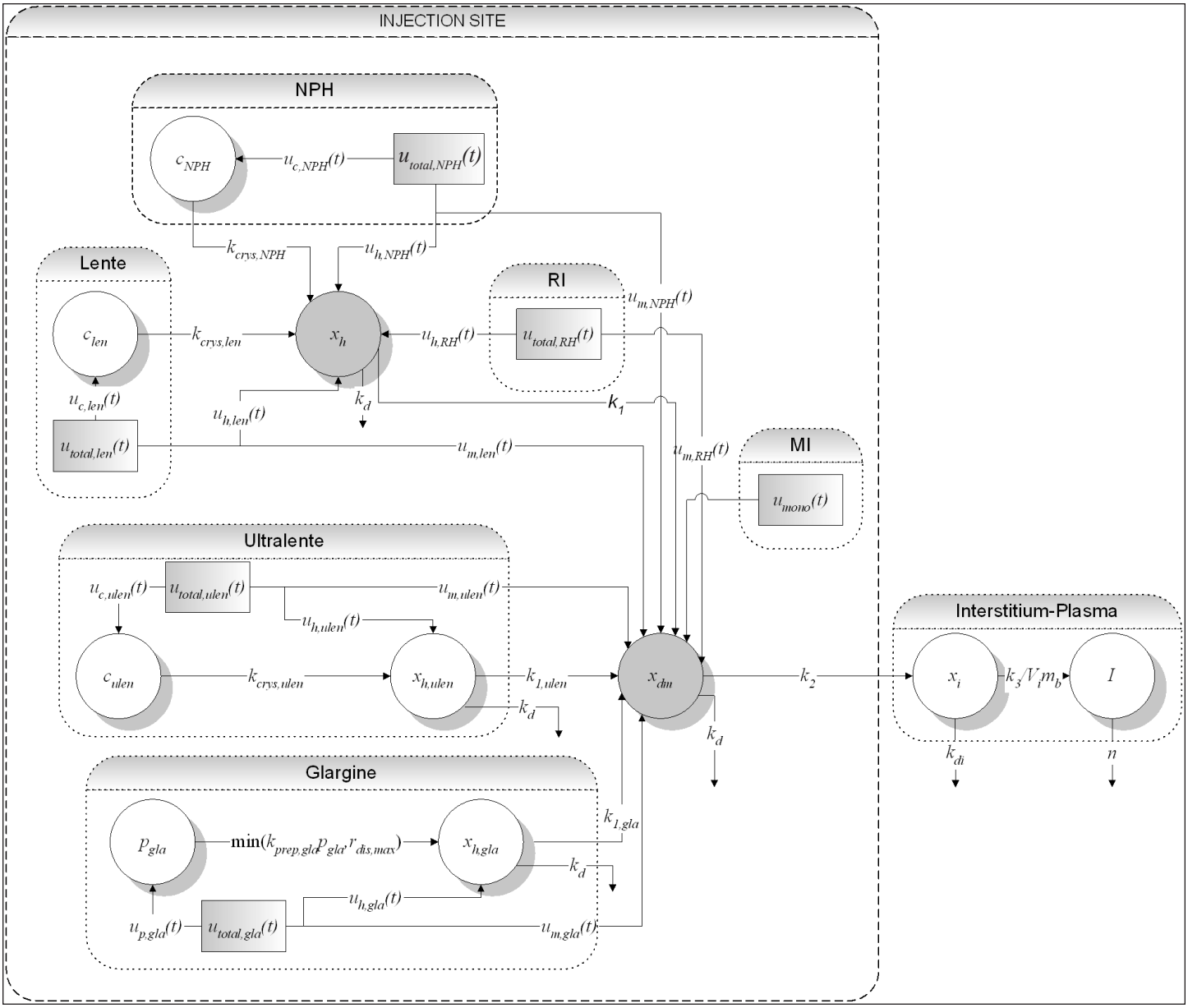


**Figure 1**. Full structure of the overall SC insulin absorption kinetic model. The model is characterized by a common hexameric state compartment for RI, NPH, and lente insulins ($x_h$), whereas those for insulin glargine and ultralente ($x_{h,ulen}$ and $x_{h,gla}$) are separate. A crystalline state compartment for NPH ($c_{NPH}$), lente ($c_{len}$), and ultralente ($c_{ulen}$) insulins and a precipitate compartment for insulin glargine ($p_{gla}$) model these insulin-specific protraction mechanisms. All insulin types flow into common dimeric–monomeric state ($x_{dm}$), interstitium ($x_i$), and plasma ($I$) compartments.

$c_{len}(t)$ Mass in the lente crystalline zinc compartment (mU)

$c_{ulen}(t)$ Mass in the ultralente crystalline zinc compartment (mU)]

$p_{gla}(t)$ Mass in the glargine precipitate compartment (mU)

$x_{dm}(t)$ Mass in the dimer/monomer compartment (mU)

$u_{total,mono}(t)$ MI input (mU/min)

$u_{total,RH}(t)$ RI input (mU/min)

$u_{total,NPH}(t)$ NPH insulin input (mU/min)

$u_{total,len}(t)$ Lente insulin input (mU/min)

$u_{total,ulen}(t)$ Ultralente insulin input (mU/min)

$u_{total,gla}(t)$ Insulin glargine input (mU/min)

$\alpha_{NPH}$ Proportion of $u_{total,NPH}(t)$ in protamine crystalline state at injection

$\alpha_{len}$ Proportion of $u_{total,len}(t)$ in zinc crystalline state at injection

$\alpha_{ulen}$ Proportion of $u_{total,ulen}(t)$ in zinc crystalline state at injection

$\alpha_{gla}$ Proportion of $u_{total,gla}(t)$ precipitate insulin from at injection

$u_{c,NPH}(t)$ NPH crystalline state insulin input (mU/min)

$u_{c,len}(t)$ Lente crystalline state insulin input (mU/min)

$u_{c,ulen}(t)$ Ultralente crystalline state insulin input (mU/min)

$u_{p,gla}(t)$ Glargine precipitate state insulin input (mU/min)

$u_{h,NPH}(t)$ NPH hexamer state insulin input (mU/min)

$u_{h,len}(t)$ Lente hexamer state insulin input (mU/min)

$u_{h,ulen}(t)$ Ultralente hexamer state insulin input (mU/min)

$u_{h,gla}(t)$ Glargine hexamer state insulin input (mU/min)

$u_{mono}(t)$ MI dimer/monomer state insulin input (mU/min)

$u_{m,RH}(t)$ RI dimer/monomer state insulin input (mU/min)

$u_{m,NPH}(t)$ NPH dimer/monomer state input (mU/min)

$u_{m,len}(t)$ Lente dimer/monomer state insulin input (mU/min)

$u_{m,ulen}(t)$ Ultralente dimer/monomer state insulin input (mU/min)

$u_{m,gla}(t)$ Glargine dimer/monomer state insulin input (mU/min)

$k_{crys,NPH}$ NPH protamine crystalline dissolution rate ($min^{-1}$)

$k_{crys,len}$ Lente zinc crystalline dissolution rate ($min^{-1}$)

$k_{crys,ulen}$ Ultralente zinc crystalline dissolution rate ($min^{-1}$)

$k_{prep,gla}$ Glargine precipitate dissolution rate ($min^{-1}$)

$V_{inj}$ Insulin dose injection volume (ml or $cm^3$)

$n$ Plasma insulin rate of clearance ($min^{-1}$)

$r_{dis,max}$ Maximum glargine precipitate dissolution rate (mU/min)

$k_1$ Hexamer dissociation rate ($min^{-1}$)

$k_{1,ulen}$ Ultralente hexamer dissociation rate ($min^{-1}$)

$k_{1,gla}$ Glargine hexamer dissociation rate ($min^{-1}$)

$k_2$ Dimeric/monomeric insulin transport rate into interstitium ($min^{-1}$)

$k_3$ Interstitium insulin transport rate into plasma ($min^{-1}$)

$k_{d,i}$ Rate of loss from interstitium ($min^{-1}$)

$k_d$ Rate of diffusive loss from hexameric and dimeric/monomeric state compartments ($min^{-1}$)

### *Regular Insulin Submodel Structure*

The RI model [**Equations 1** and **2**] is based on insulin physicochemical properties.[13] For soluble human insulins, it is generally accepted that the dynamic equilibrium of the hexameric, dimeric, and bound states characterizes absorption kinetics.[32,41–43] The equilibrium is concentration dependent and is destabilized by dilution and diffusion in the SC depot.[13,44] Qualitatively, the monomeric state has the highest absorption rate into plasma[32] and becomes increasingly stable toward the end of the absorption process when insulin concentration at the site decreases.

For simplicity, the dimeric and monomeric states are lumped in $x_{dm}(t)$ [see **Equation 2**]. Both states have higher relative absorption rates into plasma than the hexameric state, although the dimer is absorbed discernibly slower than the monomer.[32] There is no provision for a reversible, bound state.[13] However, for many common concentrations of insulin preparation, insulin binding has been shown to be negligible.[37] Reversible binding also becomes apparent only at low doses and concentrations.[13] This result implies that the effect of insulin binding is relatively small, especially when large prandial injections are administered, and might be ignored for decision support.

Thus, the RI input [**Equation 13**] is assumed to consist of hexameric, $x_h(t)$, and dimeric/monomeric, $x_{dm}(t)$, states according to the equilibrium of **Equation 33**,[13] but only at the $t$=0 injection [see **Equation 24**].

$$C_h = Q_D C_D^3 \tag{23}$$

$$\frac{u_h(t=0)}{V_{inj}} = Q_D\left(\frac{u_{dm}(t=0)}{V_{inj}}\right)^3 \tag{24}$$

where

$C_h$ Concentration of hexameric insulin [(liter/mU)$^2$]

$C_D$ Concentration of dimeric insulin [(liter/mU)$^2$]

$Q_D$ Hexameric–dimeric equilibrium constant [(liter/mU)$^2$]

$V_{inj}$ Insulin dose injection volume (ml or cm$^3$)

$u_m(t)$ Dimer/monomer state insulin input (mU/min)

$u_h(t)$ Hexamer state insulin input (mU/min)

This equation is an acknowledged simplification of the hexameric–dimeric state dynamic equilibrium, while still accounting for dose and concentration effects. Assuming a spherical depot, volume effect is modeled by a rate of diffusive loss, $k_d$, from both $x_h(t)$ and $x_{dm}(t)$ compartments in the SC depot [**Equations 25** and **26**].

$$k_d = \frac{3D}{r^2} \tag{25}$$

$$r = \left(\frac{3}{4}\frac{V_{inj}}{\pi}\right)^{\frac{1}{3}} \tag{26}$$

where

$k_d$ Rate of diffusive loss from hexameric and dimeric/monomeric state compartments (min$^{-1}$)

$D$ Diffusion constant of hexameric and dimeric/monomeric insulin (cm$^2$/min)

$r$ Radius of the SC depot (cm)

$V_{inj}$ Insulin dose injection volume (ml or cm$^3$)

Both hexameric and dimeric/monomeric states are assumed to have the same diffusion constant, a further simplification of the absorption process that was also made by Mosekilde and associates.[13]

### *Neutral Protamine Hagedorn, Lente, and Ultralente Insulin Submodel Structures*

The NPH, lente, and ultralente insulin submodel structures are similar to the RI model with an additional crystalline state compartment [**Equations 1–6**]. The crystalline state accounts for the protraction mechanism. Specifically, the formation of protamine [NPH, $x_{c,NPH}(t)$] or zinc crystals [lente, $x_{c,len}(t)$ and ultralente, $x_{c,ulen}(t)$] delays the dissolution process[20,45] [**Equations 3, 4** and **6**]. These states then flow into the hexameric state after dissolution.

Compared to RI injection [**Equation 13**], a large proportion of the injected dose is crystalline [$u_{c,NPH}(t)$, $u_{c,len}(t)$, and $u_{c,ulen}(t)$], while the rest consists of hexameric [$u_{h,NPH}(t)$, $u_{h,len}(t)$, and $u_{h,ulen}(t)$] and dimeric/monomeric states [$u_{m,NPH}(t)$, $u_{m,len}(t)$, and $u_{m,ulen}(t)$] [**Equations 9–11**, **(15)–(17)**, **(19)–(21)**]. Both the NPH and the lente insulin models incorporate the common hexameric state compartment as RI, $x_h(t)$ [**Equation 1**], while a separate, slower hexameric state is introduced for ultralente insulin, $x_{h,ulen}(t)$ [**Equation 5**].

### *Insulin Glargine Submodel Structure*

The insulin glargine model structure has several key differences to the NPH, lente, and ultralente models [**Equations 7** and **8**]. The model structure consists of a precipitate compartment, $p_{gla}(t)$ [**Equation 8**], similar in purpose to the crystalline state compartment for NPH and zinc-based insulins. Like the formation of crystals, the formation of an amorphous microprecipitate in neutral SC tissue is the primary protraction mechanism of insulin glargine, which has an acidic isoelectric point.[46] An empirical approximation is used to model the maximum dissolution rate, $r_{dis,max}$, of the precipitate [**Equations 27** and **28**] into a hexameric form unique to glargine, $x_{h,gla}(t)$.

$$r_{dis,\max}(t) = \sum_{i=1}^{N} r_{dis,\max_i}\left(H(t-t_{i-1}) - H(t-t_i)\right) \tag{27}$$

$$r_{dis,\max_i} = r_{dis,\max}(t_i < t < t_{i+1}) = \begin{cases} 15 & \text{if } u_{p,gla}(t_i) < 30{,}000 \\ 15\left(\dfrac{u_{p,gla}(t_i)}{30{,}000}\right) & \text{if } u_{p,gla}(t_i) \geq 30{,}000 \end{cases} \tag{28}$$

where $H(t - t_i)$ is the Heaviside function defined as $H(t - t_i) = 0$ when $t$ is less than $t_i$, and $H(t - t_i) = 1$ when $t$ is greater than or equal to $t_i$.

Thus, $r_{dis,max}$ is a function of dose size for doses >30 units and is a constant 15 mU/min for doses <30 units. This function has been selected based on the following model identification of the model parameters in this research. The glargine insulin hexamer is also strengthened to reduce dissociation,[46–48] resulting in greater stability in this state. This behavior is modeled using a separate hexameric state compartment $x_{h,gla}(t)$ with a different hexameric dissociation ($k_{prep,gla}$) rate to the ones used for the intermediate ($k_{crys,len}$, $k_{crys,NPH}$) and zinc-based long-acting insulin ($k_{crys,ulen}$) [see **Equation 7**]. Thus, insulin glargine is injected in a mixture of precipitate [$u_{p,gla}(t)$], glargine hexameric [$u_{h,gla}(t)$], and dimeric/monomeric states [$u_{m,gla}(t)$] [**Equations 12**, **28**, and **22**]. Its rate of diffusive loss from hexameric and dimeric/monomeric states, $k_d$, remains the same as for RI.

### *Monomeric Insulin Submodel Structure*

The MI model structure follows from the RI model structure in that the MI dose is assumed to be injected

$[u_{mono}(t)]$ entirely into the dimeric/monomeric $[x_{dm}(t)]$ compartment as 100% dimers/monomers [**Equation 14**] and is immediately available for absorption into the interstitium after injection [**Equation 2**]. Thus, the absorption kinetics of MI injection is concentration independent, unlike RI,[49,50] and is effectively a three-pool model identical to the model of Shimoda and colleagues1[7] [**Equations 2**, **29**, and **30**].

### *Interstitium and Plasma Insulin Model Structure*

From the dimeric/monomeric state, insulin diffuses into interstitium, $x_i(t)$ [**Equation 29**], and subsequently into plasma, $I(t)$ [**Equation 30**]. Plasma insulin is represented by the widely accepted one-pool model[17,28,30,31,51] in **Equation 30**.

$$\dot{x}_i(t) = -(k_3 + k_{d,i})x_i(t) + k_2 x_{dm}(t) \quad (29)$$

$$\dot{I}(t) = -nI(t) + k_3\left(\frac{x_i(t)}{V_i m_b}\right) \quad (30)$$

where

$x_i(t)$ Mass in the interstitium compartment (mU)

$I(t)$ Plasma insulin concentration (mU/liter)

$V_i$ Insulin plasma distribution volume (liter/kg)

$m_b$ Body mass (kg)

$k_{d,i}$ Rate of loss from interstitium ($min^{-1}$)

### *Summary of Model Structure*

The total model structure consists of 10 compartments with 16 parameters for six SC injected insulin types. Each insulin submodel involves no more than 2 to 3 exclusive compartments and parameters, and each individual submodel is computationally modest as a result. The model structure is integrated in that all insulin types eventually emerge in the common, physiologically expected dimeric/monomeric state prior to transport into the interstitium and plasma [**Equations 2**, **29**, and **30**]. Except for the specific insulin glargine and ultralente insulin cases, the RI, NPH, and lente insulin types similarly share one hexameric state compartment with the same transport rates [**Equation 1**].

Increased NPH and lente duration of action is described by the formation of the crystalline state only [**Equations 3** and **4**]. Increased action duration of ultralente insulin and insulin glargine are modeled both by formation of the crystalline/precipitate state and by a more stable, slower dissociating hexamer [**Equations 5–8**]. The use of crystalline and precipitate compartments is physiological, but highly simplified compared to nonlinear noncompartmental approaches.[13,37,38]

First-order transport rates are used except where *in vivo* knowledge is unpublished or unknown. In this case, empirical assumptions were made as in the case of the dose response of insulin glargine [**Equations 27** and **28**]. In this particular case, the empirical approximation is based on observations during model identification, as presented in this study.

While the absorption processes, i.e., dissolution, dissociation, and diffusion, are two way, only the net flow to plasma is modeled. This approach is another acknowledged simplification from other more complex models. It is similar to the recent compartment model of Clausen and colleagues[52] for a biphasic protamine-retarded MI–MI preparation. This particular model also has a similar crystalline state compartment and models only net flows, but with no hexameric state due to the use of MI.

## Model Parameter Identification

Certain model parameters are fixed to values in the literature and used as patient-independent population values (**Table 1**). All remaining parameters for all insulin types are patient specific and identified with nonlinear least squares (NLS) and unconstrained nonlinear optimisation methods. Data utilized are taken from 37 sets of plasma insulin time-course absorption curves (**Table 2**).

Data were collected via a literature review of relevant insulin PK studies searched in the MEDLINE and Science Citation Index Expanded (SCI-EXPANDED) databases. Only studies using direct measurement methods were considered[53] with data generally in the form of mean plasma insulin time-course measurements. These studies differ widely in cohort studied, methods, and protocol. However, data suffice for this study where the goal was

**Table 1.**
**Fixed Mode Parameters to Literature**

| Parameter | Value | Reference |
|---|---|---|
| $V_i$ | 0.1421 (liter/kg) | 15 |
| $n$ | 0.16 ($min^{-1}$) | 51 |
| $k_{d,i}$ | 0.0029 ($min^{-1}$) | 17 |
| $D$ | 0.9e-4 ($cm^2$/min) | 13 |
| $Q_d$ | 1.5e-12 [(liter/mU)$^2$] | 13 |

to develop a mean PK simulation model for a diabetes decision support system. Rather than limiting the parameter identification to a specific cohort, experimental method, and/or protocol, a parameter fit across a broad range of studies is felt to be likelier to result in an averaged PK response suitable for clinical use over the similarly wide population encountered in the general diabetes control problem.

Several major factors may affect data used for parameter identification. First, insulin antibodies may not be quantified and/or cannot be presumed negligible. This problem is an issue more with IDDM study cohorts with an extended history of diabetes that have been or are being treated using older, highly immunogenic insulin types, e.g., porcine insulin. If the cohort is not naive to the specific insulin used, insulin antibodies can significantly affect the plasma insulin concentration measurement.

Insulin antibodies generally affect plasma insulin appearance proportionately, leading to inaccurate insulin distribution volume assumptions.[28] However, in a model-based diabetes decision support system where effective insulin sensitivity is optimized in real time,[51,54] a trade-off between effective insulin sensitivity and insulin distribution volume can occur.[55,56] In this case, the shape of the plasma insulin curve is more critical within reasonable bounds than its exact magnitude.[55]

Second, endogenous insulin production may not be corrected or be presumed negligible. This determination is typically performed using C-peptide measurements for noninsulin-dependent diabetes mellitus or normal study cohorts. In most cases, however, administered doses are sufficient to suppress endogenous insulin production, and its effect may largely be disregarded when using a large number of studies for an average identification.

Finally, in the case of insulin analogues, especially insulin glargine, or animal-based insulins, insufficient cross-reactivity with a nonspecific insulin assay may result in underestimated plasma insulin concentrations. With respect to these concerns, all studies are specifically identified in **Table 2** where insulin antibodies and endogenous insulin production are accounted for. Similarly, if cross-reactivity with the insulin assay of the study insulin is sufficient. If concentration of the insulin preparation is not quoted, a typical concentration of 100 U/ml is assumed. If the insulin dose is quoted in units per kilogram, a body weight of 80 kg is assumed if no other information is provided. All of these assumptions are indicated where made and illustrate the lack of full data reporting that can often occur.

The model is built essentially by extensions from the MI model structure (**Figure 1**), which is identical to the one by Shimoda *et al.*[17] and similar to the ones by Kraegen and Chisholm[29] and Puckett and Lightfoot.[31] Equivalent parameter values from Shimoda and colleagues[17] were thus able to be used as starting points for NLS optimization of $k_2$ and $k_3$ to MI studies data (**Table 3**). With fixed population values of $k_2$ and $k_3$ identified from MI data, a two-stage NLS optimization is used to optimize $k_1$, $k_2$, and $k_3$ using data from RI studies (**Table 4**). Note that the overall fitted $k_2$ and $k_3$ values for RI data (**Table 4**) are very close to the fitted $k_2$ and $k_3$ to MI data (**Table 3**) and that all fitted parameters display a low coefficient of variation (CV) as summarized in **Table 9**. Hence, the $k_2$ and $k_3$ parameters are consistent in describing these common physiological states during the SC insulin absorption process even among different insulin types.

Referring to **Figure 1**, two parameters each must be identified for the NPH ($k_{crys,NPH}$ and $\alpha_{len}$) and lente insulin ($k_{crys,len}$ and $\alpha_{NPH}$) data set, where fixed population $k_1$, $k_2$, and $k_3$ values from RI and MI data parameter identification are used. Likewise, three parameters must each be fitted for the ultralente ($k_{crys,ulen}$, $k_{1,ulen}$, and $\alpha_{ulen}$) and insulin glargine ($k_{prep,gla}$, $k_{1,gla}$, and $\alpha_{gla}$) data sets using the same fixed $k_1$, $k_2$, and $k_3$ population values.

Because of the larger number of data sets, parameters for the NPH, lente, ultralente, and insulin glargine submodels are fitted via unconstrained nonlinear optimization using a simplex search method for multiple variables, which is a quicker method. The objective function is the plasma

**Table 3.**
**Fitted $k_2$ and $k_3$ to Published MI PK Data**

| Parameter | Reference | | | | Median | Mean (SD) | CV (%) |
|---|---|---|---|---|---|---|---|
| | 57 | 17 | 58 | 59 | | | |
| $k_2$ (min$^{-1}$) | 0.0106 | 0.0085 | 0.0119 | 0.0106 | 0.0106 | 0.0104 (0.0014) | 14 |
| $k_3$ (min$^{-1}$) | 0.0473 | 0.0752 | 0.0355 | 0.0876 | 0.0613 | 0.0614 (0.0241) | 39 |

**Table 2.**
**Published PK Studies Used for Model Parameter Identification**

| Insulin type | Dose | Concentration (U/ml) | Cohort studied[a] | Reference |
|---|---|---|---|---|
| MI | 7.1 ± 1.3 U | 100 | T1 DM | 57[b,c,d] |
| MI | 0.12 U/kg | 4 | IDDM | 17[b,c,d] |
| MI | 10 U | 100 | T1 DM | 58[b,d] |
| MI | 0.05 U/kg | 100 | Normals | 59[d] |
| RI (porcine) | 0.15 U/kg (6–9 U) | 40 | IDDM / NIDDM | 28[b,c] |
| RI | 0.1 U/kg | — | Normals | 60 |
| RI (porcine) | 10 U (rapid SC delivery) | 3.3 | Normals | 29[b] |
| RI (porcine) | 10 U (rapid SC delivery) | 40 | Normals | 29[b] |
| RI | 0.12 U/kg | 4 | IDDM | 17[b,c] |
| RI | 12 U | 100 | IDDM | 61[b] |
| RI | 10 U | — | Normals | 2 |
| RI | 15 U | 40 | Normals | 62[b] |
| RI | 15 U | 100 | Normals | 62[b] |
| RI | 6 U | 99 | Normals | 63 |
| RI (porcine) | 0.25 U/kg | — | Normals | 4[c,d] (NPH study) |
| RI (porcine) | 0.25 U/kg | — | Normals | 4[c,d] (Lente study) |
| NPH | 0.15 U/kg | 100 | Normals | 64[b] |
| NPH | 0.3 U/kg | 100 | T1 DM | 23[b] |
| NPH | 0.4 U/kg | — | Normals | 21[b] (clamp 1) |
| NPH | 0.4 U/kg | — | Normals | 21[b] (clamp 2) |
| NPH | 15 U | 40 | Normals | 62[b] |
| NPH | 15 U | 100 | Normals | 62[b] |
| NPH | 0.4 U/kg | 40 | Normals | 65 |
| NPH | 14 U | 95 | Normals | 63 |
| NPH | 0.25 U/kg | — | Normals | 4[c,d] |
| NPH | 0.4 U/kg | 86.4 | Normals | 66[c] |
| Lente | 0.25 U/kg | — | Normals | 4[c,d] |
| Ultralente | 0.4 U/kg | — | Normals | 21[b] (clamp 1) |
| Ultralente | 0.4 U/kg | — | Normals | 21[b] (clamp 2) |
| Ultralente | 0.3 U/kg | 40 | T1 DM | 23[b] |
| Ultralente | 0.3 U/kg | 100.5 | Normals | 67[b] |
| Glargine | 0.3 U/kg | 100 | T1 DM | 23[b,d] |
| Glargine | 0.15 U/kg | 100 | Normals | 64[b,d] (15 µg/ml zinc) |
| Glargine | 0.15 U/kg | 100 | Normals | 64[b,d] (80 µg/ml zinc) |
| Glargine | 0.4 U/kg | 86.4 | Normals | 66[c] |
| Glargine | 0.4 U/kg | — | Normals | 21[c] (clamp 1) |
| Glargine | 0.4 U/kg | — | Normals | 21[b] (clamp 2) |

[a] T1 DM, type 1 diabetes mellitus; IDDM, insulin-dependent diabetes mellitus; NIDDM, noninsulin-dependent diabetes mellitus.
[b] Corrected for endogenous glucose production, suppressed by protocol, or justified negligible by baseline C-peptide measurements (usually for NIDDM and normal cohorts only).
[c] Corrected for insulin antibodies or justified negligible by measurement (usually for IDDM cohorts only).
[d] Corrected for cross-reactivity of study insulin with insulin assay (usually insulin analogue or animal insulin studies only).

**Table 4.**
**Fitted $k_1$, $k_2$, and $k_3$ to Published RI PK Data**

| Parameter | Reference | | | | | | | | | | | | Median | Mean (SD) | CV (%) |
|---|---|---|---|---|---|---|---|---|---|---|---|---|---|---|---|
| | 28 | 60 | 29 | | 17 | 61 | 2 | 62 | | 63 | 4 | | | | |
| | | | 3.3 U/ml | 40 U/ml | | | | 40 U/ml | 100 U/ml | | NPH study | Lente study | | | |
| $k_1$ (min$^{-1}$) | 0.0565 | 0.0217 | 0.0348 | 0.0264 | 0.0275 | 0.0266 | 0.0365 | 0.0229 | 0.0148 | 0.0870 | 0.0235 | 0.0233 | 0.0250 | 0.0331 (0.0200) | 60 |
| $k_2$ (min$^{-1}$) | 0.0089 | 0.0148 | 0.0201 | 0.0205 | 0.0027 | 0.0088 | 0.0057 | 0.0086 | 0.0083 | 0.0067 | 0.0113 | 0.0104 | 0.0089 | 0.0106 (0.0054) | 51 |
| $k_3$ (min$^{-1}$) | 0.0681 | 0.0619 | 0.0581 | 0.0621 | 0.0631 | 0.0615 | 0.0744 | 0.0613 | 0.0612 | 0.0839 | 0.0616 | 0.0614 | 0.0618 | 0.0649 (0.0073) | 11 |

insulin concentration sum squared error (SSE), defined in **Equation 31** for the $j$th data set. As only mean insulin time-course data are used in this study, the variability of the mean value is neglected. Depending on the number of measurements in the calculation of the mean, the sum of the percentage measurement error would result in a wide error band around each mean value, which is of little value for model fit validation.

$$SSE_j = \sum_{i=1}^{N_j} \left( \bar{I}_{j,i} - I_j\left(t_{j,i}\right) \right)^2 \tag{31}$$

where $N_j$ is the number of plasma insulin data points in the $j$th data set, $\bar{I}_{j,i}$ is the $i$th plasma insulin concentration data point in the $j$th data set, and $I_j\left(t_{j,i}\right)$ is the modeled plasma insulin concentration for the $j$th data set at $t_{j,i}$, the time at the $i$th plasma insulin concentration data point. There are 37 data sets in total for all insulin types (4 MI, 12 RI, 10 NPH insulin, 1 lente insulin, 4 ultralente insulin, and 6 insulin glargine).

Results for the NPH, lente, ultralente, and insulin glargine parameter identifications are shown in **Tables 5–8**. Note that even with fixed population values for $k_1$, $k_2$, and $k_3$, the CV of all fitted NPH, lente, ultralente, and insulin glargine model parameters was <100%. Specifically, a median CV of 57% and a 95th percentile of 3.6–69.1% were achieved (results not shown). Referring to **Table 9**, the median CV was 51.3% (95th percentile of 3.6–60.6%) across all parameters and insulin submodels. This precision of fitted parameters is adequate given the data, and the parameters can be considered a posteriori identifiable following the definition of Wilinska and colleagues.[33]

### *Model Fit and Prediction Errors*

In **Table 10**, model fit error (both absolute and absolute percentage errors) and model prediction errors using population parameters (both absolute and absolute percentage errors) are shown. Across all insulin types, median absolute model fit errors range from 0.62 to 3.20 mU/liter and median absolute percentage model fit errors range from 10.96% for glargine to 21.42% for lente, of which there was only one data set. This figure

**Table 6.**
**Fitted $k_{crys,len}$ and $\alpha_{len}$ to Published Lente PK Data**

| Parameter | Reference |
|---|---|
| | 4 |
| $k_{crys,len}$ (min$^{-1}$) | 0.0037 |
| $\alpha_{len}$ (unitless) | 0.9447 |

**Table 5.**
**Fitted $k_{crys,NPH}$ and $\alpha_{NPH}$ to Published NPH PK Data**

| Parameter | Reference | | | | | | | | | | Median | Mean (SD) | CV (%) |
|---|---|---|---|---|---|---|---|---|---|---|---|---|---|
| | 64 | 23 | 21 | | 62 | | 65 | 63 | 4 | 66 | | | |
| | | | Clamp 1 | Clamp 2 | 40 U/ml | 100 U/ml | | | | | | | |
| $k_{crys,NPH}$ (min$^{-1}$) | 0.0018 | 0.0029 | 0.0017 | 0.0013 | 0.0015 | 0.0010 | 0.0038 | 0.0002 | 0.0004 | 0.0010 | 0.0014 | 0.0016 (0.0011) | 70 |
| $\alpha_{NPH}$ (unitless) | 0.9945 | 0.9471 | 0.9393 | 0.9501 | 0.9061 | 0.9018 | 1.0000 | 0.9386 | 0.9234 | 0.9737 | 0.9432 | 0.9475 (0.0336) | 4 |

**Table 7.**
**Fitted $k_{crys,ulen}$ to Published Ultralente PK Data**

| Parameter | Reference | | | | Median | Mean (SD) | CV (%) |
|---|---|---|---|---|---|---|---|
| | 21 | | 23 | 67 | | | |
| | Clamp 1 | Clamp 2 | | | | | |
| $k_{crys,ulen}$ (min$^{-1}$) | 0.0048 | 0.0012 | 0.0013 | 0.0012 | 0.0013 | 0.0021 (0.0018) | 84 |
| $k_{1,ulen}$ (min$^{-1}$) | 0.0015 | 0.0014 | 0.0044 | 0.0020 | 0.0018 | 0.0023 (0.0014) | 61 |
| $\alpha_{ulen}$ (unitless) | 1.0000 | 1.0000 | 0.8897 | 1.0000 | 1.0000 | 0.9724 (0.0552) | 6 |

**Table 8.**
**Fitted $k_{prep,gla}$ to Published Glargine PK Data**

| Parameter | Reference | | | | | | Median | Mean (SD) | CV (%) |
|---|---|---|---|---|---|---|---|---|---|
| | 23 | 64 | | 66 | 21 | | | | |
| | | 80 µg/ml zinc | 15 µg/ml zinc | | Clamp 1 | Clamp 2 | | | |
| $k_{prep,gla}$ (min$^{-1}$) | 0.0007 | 0.0019 | 0.0016 | 0.0005 | 0.0008 | 0.0008 | 0.0008 | 0.0011 (0.0006) | 53 |
| $k_{1,gla}$ (min$^{-1}$) | 0.0143 | 0.0018 | 0.0018 | 0.0062 | 0.0105 | 0.0124 | 0.0084 | 0.0078 (0.0054) | 69 |
| $\alpha_{gla}$ (unitless) | 0.9578 | 0.7694 | 0.9570 | 0.9426 | 0.9388 | 0.9498 | 0.9462 | 0.9192 (0.0738) | 8 |

**Table 9.**
**Summary of Parameter Identification to Published PK Data**

| Insulin type | Parameter (units) | Median | Mean (SD) | CV (%) |
|---|---|---|---|---|
| MI | $k_2$ (min$^{-1}$) | 0.0106 | 0.0104 (0.0014) | 14 |
| MI | $k_3$ (min$^{-1}$) | 0.0613 | 0.0614 (0.0241) | 39 |
| RI | $k_1$ (min$^{-1}$) | 0.0250 | 0.0331 (0.0200) | 60 |
| RI | $k_2$ (min$^{-1}$) | 0.0089 | 0.0106 (0.0054) | 51 |
| RI | $k_3$ (min$^{-1}$) | 0.0618 | 0.0649 (0.0073) | 11 |
| NPH | $k_{crys,NPH}$ (min$^{-1}$) | 0.0014 | 0.0016 (0.0011) | 70 |
| NPH | $\alpha_{NPH}$ (unitless) | 0.9432 | 0.9475 (0.0336) | 4 |
| Lente | $k_{crys,len}$ (min$^{-1}$) | 0.0037 | — | — |
| Lente | $\alpha_{len}$ (unitless) | 0.9447 | — | — |
| Ultralente | $k_{crys,ulen}$ (min$^{-1}$) | 0.0013 | 0.0021 (0.0018) | 84 |
| Ultralente | $k_{1,ulen}$ (min$^{-1}$) | 0.0018 | 0.0023 (0.0014) | 61 |
| Ultralente | $\alpha_{len}$ (unitless) | 1.0000 | 0.9724 (0.0552) | 6 |
| Glargine | $k_{prep,gla}$ (min$^{-1}$) | 0.0008 | 0.0011 (0.0006) | 53 |
| Glargine | $k_{1,gla}$ (min$^{-1}$) | 0.0084 | 0.0078 (0.0054) | 69 |
| Glargine | $\alpha_{gla}$ (unitless) | 0.9462 | 0.9192 (0.0738) | 8 |
| | | | Median (95$^{th}$ percentile) | 51.3 (3.6–60.6) |
| | | | Range | 3.6–80.4 |

**Table 10.**
**Model Fit and Model Prediction Errors**

| Insulin type | Error type (units) | Model fit [median (90% range)] | Model prediction using population parameters [median (90% range)] |
|---|---|---|---|
| MI | Absolute (mU/liter) | 1.54 (0.84–3.25) | 1.85 (0.78–3.69) |
| | Absolute percentage (%) | 13.30 (5.18–32.45) | 15.56 (5.69–41.00) |
| RI | Absolute (mU/liter) | 2.65 (0.65–7.96) | 6.49 (1.48–13.13) |
| | Absolute percentage (%) | 18.35 (5.94–43.37) | 38.95 (15.38–72.77) |
| NPH | Absolute (mU/liter) | 1.10 (0.33–2.42) | 1.57 (0.57–4.79) |
| | Absolute percentage (%) | 16.25 (4.90–36.05) | 22.70 (9.51–46.17) |
| Lente | Absolute (mU/liter) | 3.20 (1.68–6.11) | 3.20 (1.68–6.11) |
| | Absolute percentage (%) | 21.42 (13.10–58.18) | 21.42 (13.10–58.18) |
| Ultralente | Absolute (mU/liter) | 0.80 (0.36–2.19) | 1.81 (0.42–4.06) |
| | Absolute percentage (%) | 14.32 (4.75–27.99) | 31.05 (7.43–49.00) |
| Glargine | Absolute (mU/liter) | 0.62 (0.26–0.93) | 0.84 (0.38–1.31) |
| | Absolute percentage (%) | 10.96 (5.61–19.85) | 14.88 (8.43–28.68) |

is hence unaffected by the averaging effect of multiple studies and may not be accurate. To calculate the model prediction errors, the plasma insulin concentration is generated using the model and the *population* parameters identified. As expected, the more stable insulin analogues, e.g., MI and glargine, have much lower model prediction errors (13.30 and 10.96%, respectively), whereas the more variable insulins, e.g., RI (18.35%) and NPH (16.25%), have considerably higher prediction errors. The more stable insulin analogues are hence better predicted using fixed population parameter values than less stable insulin types.

## Conclusions

A simple, physiological compartmental model has been developed for computer simulation of SC injected insulin PKs for a diabetes decision support system. Most clinically current insulin types, including MI, RI, NPH, and insulin glargine, are modeled. The model accounts for concentration dependency of SC RI injection and models the dose dependency of insulin glargine absorption. In total, 13 patient-specific model parameters were fitted to 37 sets of plasma insulin mean time-course data over all insulin types from reported clinical studies. The remaining model parameters were assumed patient-independent constants and a priori identified from the literature. All fitted parameters have a coefficient of variation <100% (median 57%, 95th percentile 3.6–60.6%) and can be considered a posteriori identifiable. Hence, a model has been created based on known SC absorption kinetics and identified on a broad range of clinically reported studies. The precision in identified parameters is acceptable and the main clinically current insulin types have been modeled. Future validation of the model fit using clinical data is required.

**Funding:**

The authors thank the Tertiary Education Commission Te Amorangi Matauranga Matua Bright Futures Top Achiever Doctoral Scholarship for financial support.

**References:**

1. Binder C. Absorption of injected insulin. A clinical-pharmacological study. Acta Pharmacol Toxicol (Copenh). 1969;27 Suppl 2:1-84.
2. Berger M, Cüppers HJ, Hegner H, Jörgens V, Berchtold P. Absorption kinetics and biologic effects of subcutaneously injected insulin preparations. Diabetes Care. 1982;5(2):77-91.
3. Binder C, Lauritzen T, Faber O, Pramming S. Insulin pharmacokinetics. Diabetes Care. 1984;7(2):188-99.
4. Galloway JA, Spradlin CT, Nelson RL, Wentworth SM, Davidson JA, Swarner JL. Factors influencing the absorption, serum-insulin concentration, and blood-glucose responses after injections of regular insulin and various insulin mixtures. Diabetes Care. 1981;4(3):366-76.
5. Koivisto VA, Fortney S, Hendler R, Felig P. A rise in ambient temperature augments insulin absorption in diabetic patients. Metabolism. 1981;30(4):402-5.
6. Kølendorf K, Bojsen J, Nielsen SL. Adipose tissue blood flow and insulin disappearance from subcutaneous tissue. Clin Pharmacol Ther. 1979;25(5 Pt 1):598-604.
7. Koivisto VA, Felig P. Effects of leg exercise on insulin absorption in diabetic patients. N Engl J Med. 1978;298(2):79-83.
8. Klemp P, Staberg B, Madsbad S, Kølendorf K. The insulin absorption from subcutaneous tissue in smoking diabetic. Acta Endocrinol. 1982;100:37.
9. Klemp P, Staberg B, Madsbad S, Kølendorf K. Smoking reduces insulin absorption from subcutaneous tissue. Br Med J (Clin Res Ed). 1982;284(6311):237.
10. Hildebrandt P, Sestoft L, Nielsen SL. The absorption of subcutaneously injected short-acting soluble insulin: influence of injection technique and concentration. Diabetes Care. 1983;6(5):459-62.
11. de Meijer PH, Lutterman JA, van Lier HJ, van't Laar A. The variability of the absorption of subcutaneously injected insulin: effect of injection technique and relation with brittleness. Diabet Med. 1990;7(6):499-505.
12. Hildebrandt P. Subcutaneous absorption of insulin in insulin-dependent diabetic patients. Influence of species, physicochemical properties of insulin and physiological factors. Dan Med Bull. 1991;38(4):337-46.
13. Mosekilde E, Jensen KS, Binder C, Pramming S, Thorsteinsson B. Modeling absorption kinetics of subcutaneous injected soluble insulin. J Pharmacokinet Biopharm. 1989;17(1):67-87.
14. Heinemann L, Weyer C, Rauhaus M, Heinrichs S, Heise T. Variability of the metabolic effect of soluble insulin and the rapid-acting insulin analog insulin aspart. Diabetes Care. 1998;21(11):1910-4.
15. Lehmann ED, Deutsch T. A physiological model of glucose-insulin interaction in type 1 diabetes mellitus. J Biomed Eng. 1992;14(3):235-42.
16. Hovorka R, Canonico V, Chassin LJ, Haueter U, Massi-Benedetti M, Orsini Federici M, Pieber TR, Schaller HC, Schaupp L, Vering T, Wilinska ME. Nonlinear model predictive control of glucose concentration in subjects with type 1 diabetes. Physiol Meas. 2004;25(4):905-20.
17. Shimoda S, Nishida K, Sakakida M, Konno Y, Ichinose K, Uehara M, Nowak T, Shichiri M. Closed-loop subcutaneous insulin infusion algorithm with a short-acting insulin analog for long-term clinical application of a wearable artificial endocrine pancreas. Front Med Biol Eng. 1997;8(3):197-211.
18. Andreassen S, Benn JJ, Hovorka R, Olesen KG, Carson ER. A probabilistic approach to glucose prediction and insulin dose adjustment: description of metabolic model and pilot evaluation study. Comput Methods Programs Biomed. 1994;41(3-4):153-65.
19. Heise T, Nosek L, Rønn BB, Endahl L, Heinemann L, Kapitza C, Draeger E. Lower within-subject variability of insulin detemir in comparison to NPH insulin and insulin glargine in people with type 1 diabetes. Diabetes. 2004;53(6):1614-20.

20. Guerci B, Sauvanet JP. Subcutaneous insulin: pharmacokinetic variability and glycemic variability. Diabetes Metab. 2005;31(4 Pt 2): 4S7-4S24.

21. Scholtz HE, Pretorius SG, Wessels DH, Becker RH. Pharmacokinetic and glucodynamic variability: assessment of insulin glargine, NPH insulin and insulin ultralente in healthy volunteers using a euglycaemic clamp technique. Diabetologia. 2005;48(10):1988-95.

22. Heinemann L. Variability of insulin absorption and insulin action. Diabetes Technol Ther. 2002;4(5):673-82.

23. Lepore M, Pampanelli S, Fanelli C, Porcellati F, Bartocci L, Di Vincenzo A, Cordoni C, Costa E, Brunetti P, Bolli GB. Pharmacokinetics and pharmacodynamics of subcutaneous injection of long-acting human insulin analog glargine, NPH insulin, and ultralente human insulin and continuous subcutaneous infusion of insulin lispro. Diabetes. 2000;49(12):2142-8.

24. Evans JM, Newton RW, Ruta DA, MacDonald TM, Stevenson RJ, Morris AD. Frequency of blood glucose monitoring in relation to glycaemic control: observational study with diabetes database. BMJ. 1999;319(7202):83-6.

25. Schütt M, Kern W, Krause U, Busch P, Dapp A, Grziwotz R, Mayer I, Rosenbauer J, Wagner C, Zimmermann A, Kerner W, Holl RW; DPV Initiative. Is the frequency of self-monitoring of blood glucose related to long-term metabolic control? Multicenter analysis including 24,500 patients from 191 centers in Germany and Austria. Exp Clin Endocrinol Diabetes. 2006;114(7):384-8.

26. Berger M, Rodbard D. Computer simulation of plasma insulin and glucose dynamics after subcutaneous insulin injection. Diabetes Care. 1989;12(10):725-36.

27. Lehmann ED. AIDA: a computer-based interactive educational diabetes simulator. Diabetes Educ.1998;24:341.

28. Kobayashi T, Sawano S, Itoh T, Kosaka K, Hirayama H, Kasuya Y. The pharmacokinetics of insulin after continuous subcutaneous infusion or bolus subcutaneous injection in diabetic patients. Diabetes. 1983;32(4):331-6.

29. Kraegen EW, Chisholm DJ. Insulin responses to varying profiles of subcutaneous insulin infusion: kinetic modelling studies. Diabetologia. 1984;26(3):208-13.

30. Furler SM, Kraegen EW. Quantitative aspects of subcutaneous insulin absorption. Diabet Med. 1989;6(8):657-65.

31. Puckett WR, Lightfoot EN. A model for multiple subcutaneous insulin injections developed from individual diabetic patient data. Am J Physiol. 1995;269(6 Pt 1):E1115-24.

32. Kang S, Brange J, Burch A, Vølund A, Owens DR. Subcutaneous insulin absorption explained by insulin's physicochemical properties. Evidence from absorption studies of soluble human insulin and insulin analogues in humans. Diabetes Care. 1991;14(11):942-8.

33. Wilinska ME, Chassin LJ, Schaller HC, Schaupp L, Pieber TR, Hovorka R. Insulin kinetics in type-1 diabetes: continuous and bolus delivery of rapid acting insulin. IEEE Trans Biomed Eng. 2005;52(1):3-12.

34. Pham M. Diabetes: proprietary survey on insulin pumps and continuous blood glucose monitoring. New York: HSBC Securities (USA) Inc.; 2005.

35. Centers for Disease Control and Prevention. National diabetes fact sheet: general information and national estimates on diabetes in the United States, 2005. Atlanta, GA: U.S. Department of Health and Human Services, Centers for Disease Control and Prevention; 2005.

36. Lehmann ED, Deutsch T. AIDA2: A Mk. II automated insulin dosage advisor. J Biomed Eng. 1993;15:201-11.

37. Trajanoski Z, Wach P, Kotanko P, Ott A, Skraba F. Pharmacokinetic model for the absorption of subcutaneously injected soluble insulin and monomeric insulin analogs. Biomed Tech (Berl). 1993;38(9):224-31.

38. Tarín C, Teufel E, Picó J, Bondia J, Pfleiderer HJ. Comprehensive pharmacokinetic model of insulin glargine and other insulin formulations. IEEE Trans Biomed Eng. 2005;52(12):1994-2005.

39. Nucci G, Cobelli C. Models of subcutaneous insulin kinetics. A critical review. Comput Methods Programs Biomed. 2000;62(3):249-57.

40. Carson ER, Cobelli C. Modelling methodology for physiology and medicine. San Diego: Academic Press; 2001.

41. Brange J, Ribel U, Hansen JF, Dodson G, Hansen MT, Havelund S, Melberg SG, Norris F, Norris K, Snel L, *et al.* Monomeric insulins obtained by protein engineering and their medical implications. Nature. 1988;333(6174):679-82.

42. Brange J, Owens DR, Kang S, Vølund A. Monomeric insulins and their experimental and clinical implications. Diabetes Care. 1990;13(9):923-54.

43. Blundell TL, Dodson G, Hodgkin D, Mercola D. Insulin: the structure in the crystal and its reflection in chemistry and biology. Adv Protein Chem. 1972;26:279-402.

44. Emdin SO, Dodson GG, Cutfield JM, Cutfield SM. Role of zinc in insulin biosynthesis. Some possible zinc-insulin interactions in the pancreatic B-cell. Diabetologia. 1980;19(3):174-82.

45. Gin H, Hanaire-Broutin H. Reproducibility and variability in the action of injected insulin. Diabetes Metab. 2005;31(1):7-13.

46. Brange J, Vølund A. Insulin analogs with improved pharmacokinetic profiles. Adv Drug Deliv Rev. 1999;35(2-3):307-335.

47. Gerich JE. Insulin glargine: long-acting basal insulin analog for improved metabolic control. Curr Med Res Opin. 2004;20(1):31-7.

48. Campbell RK, White JR, Levien T, Baker D Insulin glargine. Clin Ther. 2001;23(12):1938-57.

49. Woodworth J, Howey D, Bowsher R, Lutz S, Santa P, Brady P. [Lys(B28), Pro(B29)] human insulin (K)--dose-ranging vs humulin R (H). Diabetes. 1993;42:A54.

50. Kaku K, Matsuda M, Urae A, Irie S. Pharmacokinetics and pharmacodynamics of insulin aspart, a rapid-acting analog of human insulin, in healthy Japanese volunteers. Diabetes Res Clin Pract. 2000;49(2-3):119-26.

51. Chase JG, Shaw GM, Lin J, Doran CV, Hann C, Robertson MB, Browne PM, Lotz T, Wake GC, Broughton B. Adaptive bolus-based targeted glucose regulation of hyperglycaemia in critical care. Med Eng Phys. 2005;27(1):1-11.

52. Clausen WH, De Gaetano A, Vølund A. Within-patient variation of the pharmacokinetics of subcutaneously injected biphasic insulin aspart as assessed by compartmental modelling. Diabetologia. 2006;49(9):2030-8.

53. Heinemann L, Anderson JH Jr. Measurement of insulin absorption and insulin action. Diabetes Technol Ther. 2004;6(5):698-718.

54. Wong XW, Singh-Levett I, Hollingsworth LJ, Shaw GM, Hann CE, Lotz T, Lin J, Wong OS, Chase JG. A novel, model-based insulin and nutrition delivery controller for glycemic regulation in critically ill patients. Diabetes Technol Ther. 2006;8(2):174-90.

55. Chase JG, Shaw GM, Lin J, Doran CV, Bloomfield M, Wake GC, Broughton B, Hann C, Lotz T. Impact of insulin-stimulated glucose removal saturation on dynamic modelling and control of hyperglycaemia. IJISTA. 2004;1: 79-94.

56. Hann CE, Chase JG, Lin J, Lotz T, Doran CV, Shaw GM. Integral-based parameter identification for long-term dynamic verification of a glucose-insulin system model. Comput Methods Programs Biomed. 2005;77(3):259-70.

57. Plank J, Wutte A, Brunner G, Siebenhofer A, Semlitsch B, Sommer R, Hirschberger S, Pieber TR. A direct comparison of insulin analogs aspart and lispro in type 1 diabetic patients. Diabetes Care. 2002;25(11):2053-7.

58. Hedman CA, Lindström T, Arnqvist HJ. Direct comparison of insulin lispro and aspart shows small differences in plasma insulin profiles after subcutaneous injection in type 1 diabetes. Diabetes Care. 2001;24(6):1120-1.

59. von Mach MA, Brinkmann C, Hansen T, Weilemann LS, Beyer J. Differences in pharmacokinetics and pharmacodynamics of insulin lispro and aspart in healthy volunteers. Exp Clin Endocrinol Diabetes. 2002;110(8):416-9.

60. Cernea S, Kidron M, Wohlgelernter J, Modi P, Raz I. Comparison of pharmacokinetic and pharmacodynamic properties of single-dose oral insulin spray and subcutaneous insulin injection in healthy subjects using the euglycemic clamp technique. Clin Ther. 2004;26(12):2084-91.

61. Kang S, Creagh FM, Peters JR, Brange J, Vølund A, Owens DR. Comparison of subcutaneous soluble human insulin and insulin analogs (Aspb9,Glub27-Aspb10-Aspb28) on meal-related plasma-glucose excursions in type I diabetic subjects. Diabetes Care. 1991;14(7):571-7.

62. Hübinger A, Weber W, Jung W, Wehmeyer K, Gries FA. The pharmacokinetics of two different concentrations of short-acting insulin, intermediate-acting insulin, and an insulin mixture following subcutaneous injection. Clin Investig. 1992;70(7):621-6.

63. Davis SN, Thompson CJ, Brown MD, Home PD, Alberti KG. A comparison of the pharmacokinetics and metabolic effects of human regular and NPH insulin mixtures. Diabetes Res Clin Pract. 1991;13(1-2):107-17.

64. Owens DR, Coates PA, Luzio SD, Tinbergen JP, Kurzhals R. Pharmacokinetics of 125I-labeled insulin glargine (HOE 901) in healthy men: comparison with NPH insulin and the influence of different subcutaneous injection sites. Diabetes Care. 2000;23(6):813-9.

65. Bottermann P, Gyaram H, Wahl K, Ermler R, Lebender A. Insulin concentrations and time-action profiles of three different intermediate-acting insulin preparations in nondiabetic volunteers under glucose-controlled glucose infusion technique. Diabetes Care. 1982;5 Suppl 2:43-52.

66. Heinemann L, Linkeschova R, Rave K, Hompesch B, Sedlak M, Heise T. Time-action profile of the long-acting insulin analog insulin glargine (HOE901) in comparison with those of NPH insulin and placebo. Diabetes Care. 2000;23(5):644-9.

67. Owens DR, Vora JP, Heding LG, Luzio S, Ryder RE, Atiea J, Hayes TM. Human, porcine and bovine ultralente insulin: subcutaneous administration in normal man. Diabet Med. 1986;3(4):326-9.